Bessel Beam

Subjects: Physics, Applied
Contributor: Muhammad Ali Butt

Diffraction is a phenomenon related to the wave nature of light and arises when a propagating wave comes across an obstacle. Consequently, the wave can be transformed in amplitude or phase and diffraction occurs. Those parts of the wavefront avoiding an obstacle form a diffraction pattern after interfering with each other. In this review paper, we have discussed the topic of non-diffractive beams, explicitly Bessel beams. Such beams provide some resistance to diffraction and hence are hypothetically a phenomenal alternate to Gaussian beams in several circumstances. Several outstanding applications are coined to Bessel beams and have been employed in commercial applications. We have discussed several hot applications based on these magnificent beams such as optical trapping, material processing, free-space long-distance self-healing beams, optical coherence tomography, superresolution, sharp focusing, polarization transformation, increased depth of focus, birefringence detection based on astigmatic transformed BB and encryption in optical communication. According to our knowledge, each topic presented in this entry is justifiably explained.

Keywords: optical trapping ; material processing ; free-space long-distance self-healing beams ; optical coherence tomography ; superresolution ; sharp focusing and polarization transformation ; depth of focus

1. Introduction

In 1987, BBs were first studied by Durnin[1] and have been widely employed in applications related to both optics[2][3] and acoustics[4][5][6]. In acoustics, BBs are generally used in applications such as ultrasound imaging systems[7][8][9]. Their extended DOF and slender beam-width provide a precise scanning of the transmitted beam, whereas their self-recovering properties contribute toward extraordinary robustness to tissue scattering. Moreover, its diffraction-free feature provides a perpetual deep imaging resolution. The diffraction-free self-healing features of the BB permits it to penetrate deep into the volume of a sample, resist against refractions in chaotic environments, and provides an axial resolution as compared to that of GBs. The fields, formed from coherent mixtures of BBs, reveal a more than ten-fold rise in their undistorted penetration to diffraction-limited beams. Recently, vortex beams, to be specific, BBs, have gathered a lot of interest because of their distinctive properties for particle trapping[10][11][12][13], particle handling/rotation applications[14][15][16] or acoustic radiation force strategies in liquids[17]. BBs have also been employed in photopolymerization[18] as well as in material processing[19]. However, their prospects for high-throughput 3D printing have not been effusively investigated.

2. Optical Trapping with BBs

The techniques of tweezing and optical trapping are established on the forces that emerge as a result of the rule of momentum preservation in the reflection, refraction, and absorption of the laser beam at the particle[20][21]. For effective optical handling, i.e., consistent microparticles trapping, a high gradient of the optical power density is required. For instance, a sharply focused laser light beam is essential to trap the microparticle. This considerably shrinks the working area owing to diffraction, tighter focusing outcomes in faster radiation divergence, and the issue cannot be solved regarding the Gaussian optics. Nevertheless, Durnin[1] has demonstrated in his remarkable work that the diffractive divergence can be practically removed with a special class of non-diffracting light fields known as BBs. Practically speaking, BBs display a limited propagation length, which is dependent on the width of the original collimated beam. As the BBs preserve their focus throughout the way, the placement of the manipulated object can be considerably altered, hence allowing practical flexible micromanipulation systems. Additionally, the employment of BBs unveils novel prospects in micro-fabrication[22], manipulation of micro-machines[23] and numerous “lab-on-a-chip” applications[24].

Optical traps based on focused BBs offer highly superior capabilities for manipulation of individual glass beads in the three spatial directions in comparison with standard optical tweezers based on focused GB[25]. Interesting possibilities for the simultaneous trapping and rotating of various types of dielectric particles (with high and low refractive indexes) provide multi-ringed vortex beams[26]. The angular momentum density of BBs is similar to that of multi-ringed LG beams[27][28]. However, high-order BBs are easier to generate experimentally[29].

The field of optical trapping has grown into an essential phenomenon in the biological examination, cold atom physics, and genetics[30][31]. It has swiftly bee established from its first verification by Ashkin in the 1970s[20]. Regardless of its extensive implementation, the optical trapping of airborne particles employing a single-beam gradient-force was not verified until 1997[32]. Even nowadays, most of the laser tweezer operations are being used to trap fairly translucent specks in a liquid. A particle trapping via a single laser beam in the air is a more challenging task than in a liquid medium, as the optical trap should be robust to conquer gravity and disruption in the air. Moreover, as opposed to a particle in a liquid medium, a particle in the air has a higher relative refractive index, which induces a sturdy scattering force that tends to disrupt the trap[33]. Nevertheless, for particle delivery strategies, the potentiality to trap airborne particles is essential[34] as well as developing aerosol classification methods that incorporate optical trapping with examination practices, for instance, Raman spectroscopy[33][35].

Consequently, significant attention has been given to develop novel methods to capture airborne particles utilizing either the photophoretic force or the radiative pressure force. In recent times, the photophoretic force has been used to permit optical trapping of airborne particles with absorbing properties. Several beam shapes such as vortex beams[36], bottle beams[37], and hollow cones produced via a single beam[38], tapered rings[39], two counter-propagating beams[40] and optical lattices [41], among others, have been employed. In[36][37][38][39][40], the particles are trapped in the low-intensity area, which is contrasted to laser tweezers where the gradient force traps the particles near a laser beam's high-intensity focal point. As several photophoretic traps are only successful for particles with a specific geometry[42], the morphology of the absorbing particles poses additional technical hitches. Nevertheless, some applications include the ability to capture the particles irrespective of their construction and absorption.

An interesting method is proposed in[43], where a single formed laser beam is used to form a region of low light intensity for photophoretic trapping of absorbing particles but minimizing the dispersion force near the focal point at the same time. As a result, radiative pressure found that the trapping of translucent particles is facilitated as shown in Figure 1a–d. Besides, this low dispersion force permits airborne particles to be trapped by radiative pressure-based trapping via relatively low numerical aperture optics. A comparable method has lately been demonstrated to allow optical trapping of high relative refractive index non-absorbing particles utilized to trap airborne aerosol droplets[44].

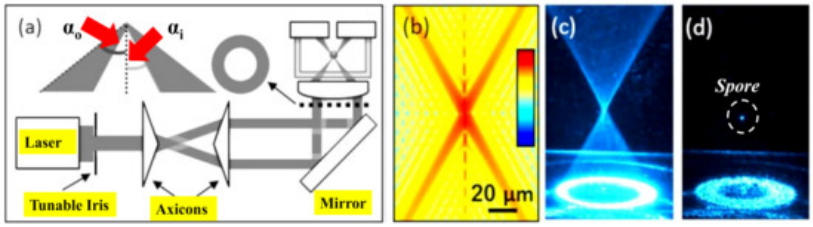

Figure 1. (**a**) Illustration of the optical trapping setup. The diameter of an expanded laser beam is managed with a tunable iris before travelling through the two axicons to form a collimated hollow beam. The aspheric lens creates a hollow conical focus within a glass chamber where airborne particles are trapped, adapted with permission from[43]. (**b**) Calculated intensity profile near the focal spot, adapted with permission from[43]. (**c**) Image of the conical focal region produced inside the chamber, adapted with permission from[43]. (**d**) Image of a spore captured in the air close to the focal point, adapted with permission from[43].

Due to the transfer of momentum from photons to particles, the radiative pressure force, the gradient force and the scattering force produced from a single laser beam emerges. Regardless of the realization of optical tweezers in maneuvering particles in the fluid, optical traps based on radiative pressure utilizing a single laser beam are still not suitable for grabbing airborne particles. Bearing in mind the radiative pressure force as an amalgamation of a gradient force and a scattering force, this problem can be solved. The gradient force drags a particle close to the focus of the laser beam into the high-intensity region at the focus, ensuring the restoring force is mandatory to catch a particle. Instead, the scattering force moves the particle in the direction of the propagation of light and off-limits the reinstating force needed. In general, optical trapping is only probable when the gradient force overpowers the dispersion force[32]. Airborne particle trapping is a challenging task due to the high refractive index of a particle in the air comparative to the ambient medium results in a sturdy scattering force. To form a robust gradient force to trap airborne particles, high numerical aperture optics (typically NA > 0.9) are obligatory[32]. In principle, by utilizing a counter-propagating beam configuration, the scattering force can be concealed[45]. However, an accurate orientation is required, which is practically not possible in many applications. If a laser light falls on absorbing airborne particles, a portion of the light is absorbed and transformed into heat. Consequently, an interplay between a non-uniformly heat-emitting particle and the ambient gas molecules leads to the photophoretic force. As a result, absorbing airborne particles are captured by the photophoretic force. For instance, if an absorbing airborne particle is hit by a light from one side, due to impact with the hot part of the particle, the gas

molecules on the elevated temperature side of the particle will have greater velocities, imposing a net force that moves the particle to its cold side. The photophoretic force can be ~5 orders of magnitude more robust than the gradient force for an intensely absorbing particle, usually employed in optical tweezers[46].

3. Material Processing via Ultrafast BBs

These days, micro- and nano-technologies rely on the growth of detailed and manageable manufacturing tools that are capable of structuring materials with full precision and minimum collateral loss. In a range of applications, from entertainment to medicine, lasers have proven to be flexible instruments over the years. The individual usage of this system is dependent on different parameters of the radiation emitted, such as wavelength, energy, and pulse duration. When considering some applications, the beam structure is essential[47][48][49]. A typical GB is appropriate for some of them. The ultra-short laser processing technique has grown into a vital technology capable of delivering fundamental processing skills well into the size of the nanoscale[50][51][52]. This counts on incomparable material processing capabilities through nonlinear excitation and inadequate thermal diffusion, resulting in high-end applications where energy localization in space and time by ultrashort pulses is important. Novel models of laser material processing are developed based on the spatiotemporal design of irradiation rendering to the material response to optimize the structuring process concerning quality and scale[53][54][55]. To synergistically associate irradiation and material reaction to energy load, an advanced processing strategy involves a detailed understanding of the irradiation and material transformation method.

For material processing applications in ultrafast modes, a new class of ultrafast laser beams has recently emerged with the potential to achieve processing precision beyond the diffraction limit, deep into the nanoscale domain. This relies on non-diffractive concepts, especially the Bessel-Gauss beam[56], where non-diffractive propagation can be used to design the multi-dimensional interaction segment. In transparent materials, the ability of these Bessel-Gauss beams is entirely utilizable, with an energy gap larger than photon energy. BBs are helpful in Bragg grating inscription[57], microchannel forming[58] and photopolymerization[59] due to an elongated focal area. BBs have a ring-shaped spatial spectrum. It is conceivable to attain Mathieu beams with elliptical intensity distribution by modifying the phase and amplitude of the BB. For instance, the elliptical beam structure has been shown to cause directional glass cracking. Zeroth and higher-order BBs are among the most distinguished non-diffracting beams and can be comprehended utilizing diffractive holograms or by focusing Laguerre GBs via conical prisms (axicons).

In[60], a novel method is developed for the realization of superimposed complex BB vortices of different orders, single and superimposed Mathieu beams of different topologies, as well as parabolic non-diffracting beams. Furthermore, their amplitudes and phases are controlled in the focal region independently to assist the creation of complex patterns not only in the transverse plane but also along the focal line. The experimental verification using a conical prism together with a geometrical phase element is presented for the transparent materials. In[61] the higher-order vector BBs are produced for transparent material processing applications.

Three-dimensional integrated circuits are an enticing option to replace standard two-dimensional ones as high-efficiency, low power exhaustion and miniaturized foot-print microelectronic devices[62]. One of the primary enduring problems, however, is the processing of high-aspect-ratio through-silicon vias (TSVs), which is a critical technology for the assembly of three-dimensional silicon integrated circuits. As a simple and environmentally friendly substitute with less manufacturing stages due to the exclusion of photolithography, TSV manufacturing through direct laser drilling has been suggested. This has been demonstrated with the production of 20 µm diameter holes in a 250 µm thick silicon substrate employing nanosecond UV laser percussion[63]. However, for the assembly of three-dimensional silicon integrated circuits, the deep drilling of holes smaller than 10 µm in diameter remains a major future challenge. Ultrafast laser treatment has recently been shown to be a desirable method for material processing, as it facilitates sub-diffraction-limit processing with heat-affected zone elimination[64]. High-quality cutting has been successfully checked for planar silicon elements with 780 nm femtosecond lasers[65]. Furthermore, in many important research and engineering applications, fast speed and high aspect ratio drilling of through-holes in different materials utilizing ultrafast laser processing have become an attention-grabbing theme. In different silica glasses, femtosecond BBs have been employed to create microstructures with aspect ratios of up to 10^{2}–10^{3}, without requiring sample transformation due to the elongated field depth.

In[66], TSVs are fabricated by using femtosecond BBs with wavelength tuning of 400 nm to 2400 nm. The manufacture of fine TSVs utilizing a 1.5 µm femtosecond BB is demonstrated in[67]. A Bessel femtosecond beam is customized via a specifically fabricated binary phase plate to remove the extreme ablation brought by the sidelobes of a traditional BB. Three separate forms of femtosecond laser beams such as a Gaussian beam (GB), a conventional BB (CBB) and a tailored BB (TBB) were used to determine the theory of the suggested method as shown in Figure 2a–c. It is established that the customized femtosecond BB (without sidelobe destruction) can be employed to form a two-dimensional periodic arrangement of ~10 µm TSVs on a silicon substrate of thickness 100 µm, indicating a possible use in the three-

dimensional assembly of three-dimensional silicon integrated circuits. Two-dimensional profiles of CBB and TBB in the x-y plane together with the on-axis intensity distributions (orange curve) are experimentally measured as displayed in Figure 2d,e, respectively. The experimentally obtained transverse intensity distributions of the CBB and TBB at $z = z_{max}$ are presented in Figure 2f,g, respectively, together with a charged coupled device taken pictures of the particular beams in the insets. Figure 2h–j illustrate the SEM pictures of the TSVs formed in 50 µm thick samples employing the GB, CBB and TBB, respectively.

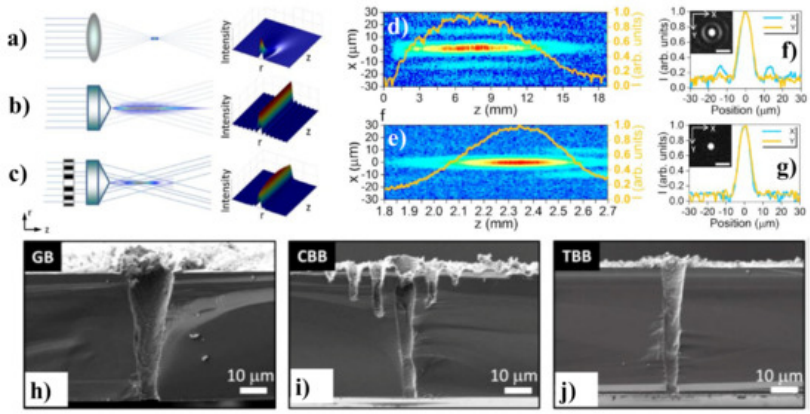

Figure 2. Diagram of the beams generation setup and intensity profiles for, (**a**) GB, (**b**) CBB and (**c**) TBB. Experimentally measured two-dimensional profiles in the x-y plane in cooperation with the on-axis intensity distribution (Orange curve) of, (**d**) CBB and (**e**) TBB. Measured transverse intensity distributions at $z = z_{max}$ along the CCD captured images of (**f**) CBB and (**g**) TBB. SEM images of the cross-sectional view of TSVs manufactured silicon substrate using (**h**) GB, (**i**) CBB and (**j**) TBB. Adapted with permission from[67].

4. Free-Space long-Distance Self-Healing BBs

In addition to the non-diffractive feature, BBs are self-healing which means that they have a self-reconstruction ability after a hurdle comes across their transmission path[68]. The intensity arrangement at z and $z + \delta_z$ is formed by different sections of the crossing planar beams as shown in Figure 3. This property comes from the selective constructive interference occurring between multiple coherent plane waves propagating at an equal angle concerning the optical axis. The redevelopment distance of the beam relies on the size of the hurdle and the angle defining the conical superposition of the planar beams. Consequently, BBs are usually more prone to dispersion than most other traditional Gaussian beams. Due to the unusual non-diffractive and self-recovery properties, BBs have gathered particular attention in biomedical physics, laser processing and metrology[69].

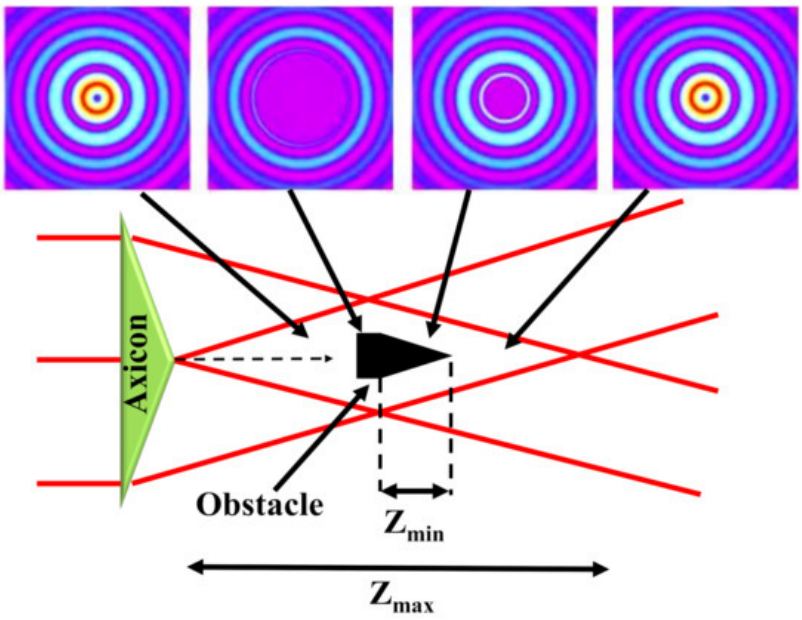

Figure 3. Self-healing features of an axicon-produced BB: an obstacle located in the center of the Bessel region blocks the beam for the smallest distance Z_{min}, the Bessel field reconstructs after travelling for some distance. The beam profiles before and after the obstacle are also shown. Inspired by[70].

A novel method for creating long-distance self-recovering BBs generated by an annular lens and a 4f-configuration spherical lens is stated in[71]. This shows the diffraction-free light evolution of a zeroth-order BBs over several meters and addresses the available scaling prospects that exceed present technologies. Additionally, it has been shown that this setup can be modified to generate BB superpositions, realizing the longest optical conveyor beam and helicon beam. Last but not least, the self-healing properties of the beams are verified concerning robust opaque and transparent scatterers, which underscores the pronounced perspective of this novel approach[71].

Underwater wireless communication is supposed to have high data rates to relay big data over several meters via a proper wavelength. It has already gained more and more recognition with a massive rise in underwater applications, for instance, unmanned underwater vehicles, submarines and sensors in the oceanic environment[72][73][74], among others. The optical turbulence is primarily caused by variations in temperature and salinity in underwater environments, such as in oceans. The standard of communication of the orbital angular momentum (OAM)-based underwater wireless communication system has been seriously impaired by this turbulence[75]. A hypothetical analysis of the effect of temperature and salinity variations on the typical strength of the Gaussian Schell-model vortex beams in the turbulent ocean has shown that partially coherent beams have a more effective resistance to turbulence than full coherent beams[76]. The transmission of partially coherent Laguerre-GBs in the tempestuous ocean is studied in[77][78]. Furthermore, the influence of the ocean instabilities on the oceanic OAM-based underwater wireless communication system's channel capacity has also been observed in[79]. In[76] [126] the statistical characteristics of the vortex beams such as the power, polarization, and coherence travelling in oceanic turbulence are theoretically studied.

Vortex beams bearing OAM with helical phase fronts have been commonly used as beam sources to mitigate the turbulence effect on any optical vortex[80]. A Bessel-Gaussian (BG) beam is an imperative part of the pseudo-non diffraction vortex beams family. In the case of blockades, BG beams can heal themselves, which is an important feature for optical communications based on the line-of-sight operations[81]. Consequently, for the OAM-based underwater communication systems[82][83], the non-diffraction and self-recovery properties of BG beams make them a valuable commodity. The transmission characteristics of BG beams in the free space environment was explored[84] and the non-obstruction characteristics of BG beams in a free-space optical communication system were studied in[85].

An experimental study of the underwater transmission and self-recovering properties of BG beams has recently been provided in[81]. A GB with a wavelength of 532 nm is transmitted from a laser diode and then a neutral density filter (NDF) is employed to reduce the intensity of the GB. The GB matches its polarization to the optimized working polarization of the selected polarization-sensitive spatial light modulator (SLM) after passing through the polarizer (Pol.) and a half-wave plate (HWP). When the polarized GB is illuminated on an SLM, the desired BG mode is generated, where the special phase hologram grating is revealed on the liquid crystal screen of the SLM. The BG beam carrying the OAM mode is then transferred through a water tank simulating the underwater environment. A rectangular water tank of one meter in length was used to replicate the underwater atmosphere. The temperature variations were regulated by a heater within the container, and salinity variations were accompanied by adding different salt bulks in the water. The experimental setup to analyze the BG beam properties underwater is shown in Figure 4a, whereas the recorded beam profiles at the receiver are shown in Figure 4b. For more detailed information, discuss[81].

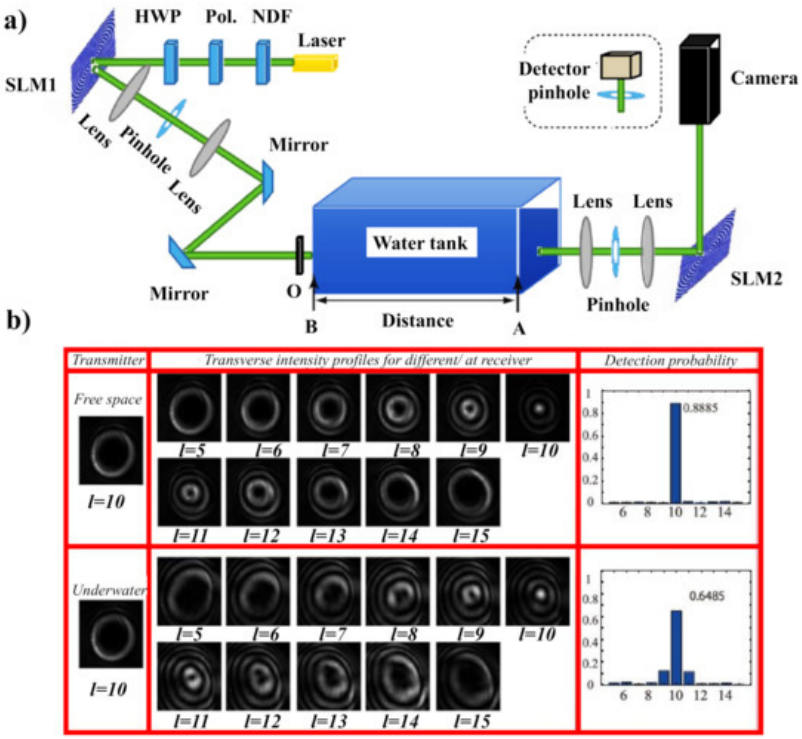

Figure 4. (**a**) The investigational arrangement for examining BG beam properties in the underwater situation. (**b**) The influence of underwater optical turbulence on the transmission of BG beam versus free space atmosphere. Adapted with permission from[81].

5. BB for Optical Coherence Tomography

Optical coherence tomography (OCT) is an imaging process that offers in situ, non-invasive, high resolution, cross-sectional pictures of the biological tissues. Given the depth of penetration of a light beam into biological tissue, endoscopic probes are needed to examine the conditions of wall linings inside the organs such as the liver, stomach, lung, colon and wider arteries within the body. Various types of endoscopic OCT systems have been developed after the first endoscopic applications of OCT in 1996[86]. Traditional GBs are currently used in endoscopic probes. Some are relocated to the targeted site by moving a wire backwards and forward in and out of the body to steer the catheter. These probe types work at the low numerical aperture and have a lateral resolution of ~20 μm. Some probes use higher numerical aperture optics; nevertheless, they are limited to the smaller DOF. A fine focus modification is needed for these probes which cannot be accomplished by wire adjustment. A gradient index (GRIN) lens rod-based probe was then demonstrated to focus on targeted points in a sample by shifting a stage out of the body[87]. Nevertheless, some endoscopic applications are constrained by the nonflexible rod. The growth of elongated DOF imaging arrangements is therefore an active research area of OCT[88]. Several methods have been applied, such as the Swept-source, time and spectral-domain OCT. Of these methods, the spectral-domain is favored over others, since it is simple to implement and does not require a complex structure. Initially, the OCT system was arranged only in free optics, but the advent of optical fiber improves the versatility of the system and paves the way for a new area of operation[89]. In OCT, the sample beam interferes with the reference beam to produce interference spectra that are further analyzed by the dedicated sample imaging tools. OCT may be achieved by either dual-path or a common-path interferometry techniques. The later methodology can solve the problems of polarization mismatch, group velocity dispersion and ambience vibration. The common path configuration eliminates device and computational complexity since there is no need for extra modules and algorithms to compensate for dispersion.

Imaging based on BB, produced by axicon optics, differs from GB imaging in that it allows the focusing range to be extended without losing resolution[90]. However, the trade-off is a reduction in the illumination and collection efficiency. OCT employing BB has become a trend to benefit from a long DOF and tighter spot size. Bessel beams for illumination/detection were used to break the limit of focus range and transversal resolution given by the GB profile[91][92][93]. The use of axicon optics in time-domain OCT was originally considered by Ding et al.[94]. Lately, a non-dual path imaging scheme for imaging of biological samples has been suggested employing Fourier-domain OCT (FD-OCT)[95]. A custom-made micro-optic axicon is used to produce a BB to lighten and image in biological samples using spectral-domain OCT (SD-OCT)[96]. Concerning the GB, BB concurrently produces a high DOF and a tight focus point. It is not possible to produce perfect BB, but the GB can be converted into a BB structure known as a Bessel-Gauss beam and is often referred to as a BB. Several methods are discussed to transform the standard GB to BB. Traditionally, the axicon

lens may be the best alternative for the transformation of the beam. A lot of impressive work has been performed on the generation of BB via the axicon lens[97][98]. However, BB axicon lens construction uses free optics, which are not appropriate for applications where there is a need for a small central spot size.

To eliminate group velocity dispersion and polarization incompatibility between the reference and the sample arm, common-path optical coherence tomography (CP-OCT) is used so that both arms share the same physical path. Current CP-OCT implementations usually involve one to incorporate an additional cover glass into the beam path of the sample arm to provide a reference signal. This step is further reduced by making direct use of the back-reflected signal, provided by the conical lens-tip fiber, as a reference signal as shown in Figure 5a[99]. The conical lens, which is directly manufactured by a simple selective-chemical etching process on the optical fiber tip (inset of Figure 8a), performs two functions: (1) it can be used as an imaging lens; (2) as the self-aligning reference plane.

Researchers have been involved in producing such axicon structures within the optical fiber such that they can be used for imaging and sensing applications. Considerable work is being conducted on BB construction using optical fibers and deep-sealed negative axicons (DSNAs) [100][101]. The DSNA is manufactured by standard chemical etching in hydrofluoric acid (HF) at the tip of the single-mode highly doped photosensitive optical fiber and produces BB[102]. A tomography methodology for fluorescence microscopy scanning is introduced in[103], which enables the volume image to be captured in a single frame scan. Volumes are photographed by concurrently recording four independent projections at various angles using temporally multiplexed, tilted BBs.

An FD-OCT method is used to exhibit the effectiveness of this method upon biological tissue. An in-fiber CP-OCT technique can prove to be potentially useful in endoscopic OCT imaging. The usefulness of employing axicon micro-optics has been solely established by imaging a biological sample, precisely an African frog tadpole, at different places attained with an incident power of 25 mW and an irradiation time of 50 µs as shown in Figure5b The detailed study on SD-OCT can be found here[96].

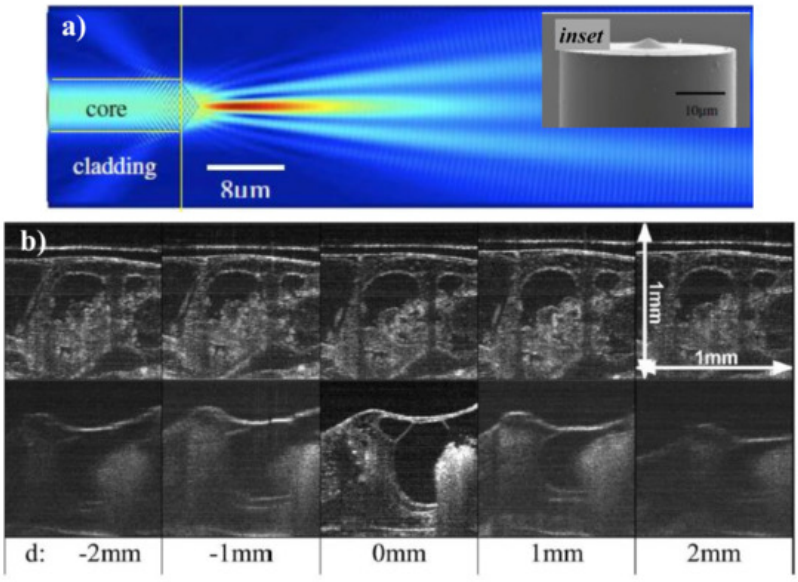

Figure 5. (**a**) Illustration of a light field travelling from the fiber to the sample and back. The inset displays the SEM image of the fiber probe where the conical microlens can be seen. Adapted with permission from[99], (**b**) 1 mm × 1 mm SD-OCT images of an African from tadpole located at various d values acquired using a 600 µm effective axicon micro-optic lens (top row) and a 0.037 NA conventional lens (bottom row). Adapted with permission from[96].

References

1. J. Durnin; Exact solutions for nondiffracting beams I The scalar theory. *Journal of the Optical Society of America A* **1987**, *4*, 651-654, 10.1364/josaa.4.000651.
2. Fahrbach, A.R.F. Propagation stability of self-constructing Bessel beams enables contrast-enhanced imaging in thick media. Nat. Commun. 2011, 3, 632.
3. Li, Z.; Alici, K.B.; Caglayan, H.; Ozbay, E. Generation of an axially asymmetric Bessel-like beam from a metallic subwavelength aperture. Phys. Rev. Lett. 2009, 102, 143901.

4. Shi, C.; Dubois, M.; Wang, Y.; Zhang, X. High-speed acoustic communication by multiplexing orbital angular momentum. Proc. Natl. Acad. Sci. USA 2017, 114, 7250–7253.
5. Jiang, X.; Liang, B.; Cheng, J.C.; Qiu, C.W. Twisted acoustic: Metasurface-enabled multiplexing and demultiplexing. Adv. Mater. 2018, 30, 1800257.
6. Marston, P. Scattering of a Bessel beam by a sphere. J. Acous. Soc. Am. 2007, 121, 753.
7. Hsu, D.; Margetan, F.; Thompson, D. Bessel beam ultrasonic transducer: Fabrication method and experimental results. Appl. Phys. Lett. 1989, 55, 2066.
8. Lu, J.-Y.; Song, T.-K.; Kinnick, R.; Greenleaf, J. In vitro and in vivo real-time imaging with ultrasonic limited diffraction beams. IEEE Trans. Med. Imaging 1993, 12, 819–829.
9. Lu, J.-Y.; Xu, X.-L.; Zou, H.; Greenleaf, J. Application of Bessel beam for doppler velocity estimation. IEEE Trans. Ultrason. Ferroelectr. Freq. Control 1995, 42, 649–662.
10. Xu, N.; Liu, G.; Kong, Z.; Tan, Q. Creation of super-resolution hollow beams with long depth of focus using binary optics. Appl. Phys. Express 2019, 13, 012003.
11. Suarez, R.; Ambrosio, L.; Neves, A.; Zamboni-Rached, M.; Gesualdi, M. Experimental optical trapping with frozen waves. Opt. Lett. 2020, 45, 2514–2517.
12. Liu, Z.; Tang, X.; Zhang, Y.; Zhang, Y.; Ma, L.; Zhang, M.; Yang, X.; Zhang, J.; Yang, J.; Yuan, L. Simultaneous trapping of low-index and high microparticles using a single optical fiber Bessel beam. Opt. Lasers Eng. 2020, 131, 106119.
13. Porfirev, A. Realisation of active pulling/pushing laser beams for light-absorbing particles in the air with a pair of diffractive optical elements. Opt. Laser Technol. 2021, 133, 106584.
14. Ali, R.; Pinheiro, F.; Dutra, R.; Maia Neto, P. Tailoring optical pulling forces with composite microspheres. Phys. Rev. A 2020, 102, 023514.
15. Voitiv, A.; Andersen, J.; Siemens, M.; Lusk, M. Optical vortex braiding with Bessel beams. Opt. Lett. 2020, 45, 1321.
16. Qiu, S.; Ren, Y.; Liu, T.; Chen, L.; Wang, C.; Li, Z.; Shao, Q. Spinning object detection based on perfect optical vortex. Opt. Lasers Eng. 2020, 124, 105842.
17. Antoine Riaud; Michael Baudoin; Jean-Louis Thomas; Olivier Bou Matar; Cyclones and attractive streaming generated by acoustical vortices. *Physical Review E* **2014**, *90*, 013008, 10.1103/physreve.90.013008.
18. Yoshihiko Arita; Jun Hyung Lee; Haruki Kawaguchi; Reimon Matsuo; Katsuhiko Miamoto; Kishan Dholakia; Takashige Omatsu; Photopolymerization with high-order Bessel light beams. *Optics Letters* **2020**, *45*, 4080-4083, 10.1364/ol.396012.
19. Alessandro Zannotti; Cornelia Denz; Miguel A. Alonso; Mark R. Dennis; Shaping caustics into propagation-invariant light. *Nat. Commun.* **2020**, *11*, 3597, .
20. Ashkin, A. Acceleration and trapping of particles by radiation pressure. Phys. Rev. Lett. 1970, 24, 156.
21. Zemanek, P.; Volpe, G.; Jonas, A.; Brzobohaty, O. Perspective on light-induced transport of particles: From optical forces to phoretic motion. Adv. Opt. Photonics 2019, 11, 577–678.
22. Jun Amako; Daisuke Sawaki; Eiichi Fujii; Microstructuring transparent materials by use of nondiffracting ultrashort pulse beams generated by diffractive optics. *Journal of the Optical Society of America B* **2003**, *20*, 2562, 10.1364/josab.20.002562.
23. Amy E. Larsen; David G. Grier; Like-charge attractions in metastable colloidal crystallites. *Nature* **1997**, *385*, 230-233, 10.1038/385230a0.
24. V. Garcés-Chávez; D. McGloin; H. Melville; W. Sibbett; K. Dholakia; Simultaneous micromanipulation in multiple planes using a self-reconstructing light beam. *Nature* **2002**, *419*, 145-147, 10.1038/nature01007.
25. Yareni A. Ayala; Alejandro V. Arzola; Karen Volke-Sepúlveda; Comparative study of optical levitation traps: focused Bessel beam versus Gaussian beams. *Journal of the Optical Society of America B* **2016**, *33*, 1060-1067, 10.1364/josab.33.001060.
26. V. Garcés-Chávez; David McGloin; Miles J. Padgett; W. Dultz; H. Schmitzer; Kishan Dholakia; Observation of the Transfer of the Local Angular Momentum Density of a Multiringed Light Beam to an Optically Trapped Particle. *Physical Review Letters* **2003**, *91*, 093602, 10.1103/physrevlett.91.093602.
27. Volke-Sepulveda, K.P.; Garces-Chavez, V.; Chavez-Cerda, S.; Arlt, J.; Dholakia, K. Orbital angular momentum of a high-order Bessel light beam. J. Opt. B Quantum Semiclassical Opt. 2002, 4, S82–S89.
28. Volke-Sepulveda, K.; Chavez-Cerda, S.; Garces-Chavez, V.; Dholakia, K. Three-dimensional optical forces and transfer of orbital angular momentum from multi-ringed light beams to spherical microparticles. J. Opt. Soc. Am. B 2004, 21,

1749–1757.

29. Svetlana Nikolaevna Khonina; V. V. Kotlyar; R. V. Skidanov; V. A. Soĭfer; Konstantins Jefimovs; J. Simonen; J. Turunen; Rotation of microparticles with Bessel beams generated by diffractive elements. *Journal of Modern Optics* **2004**, *51*, 2167-2184, 10.1080/0950034042000265569.
30. Ashkin, A.; Dziedzic, J. Optical trapping and manipulation of viruses and bacteria. Science 1987, 235, 1517–1520.
31. Neuman, K.; Block, S. Optical Trapping. Rev. Sci. Instrum. 2004, 75, 2787–2809.
32. Ryota Omori; Tamiki Kobayashi; Atsuyuki Suzuki; Observation of a single-beam gradient-force optical trap for dielectric particles in air.. *Optics Letters* **1997**, *22*, 816-818, 10.1364/ol.22.000816.
33. Jon B. Wills; Kerry J. Knox; Jonathan P. Reid; Optical control and characterisation of aerosol. *Chemical Physics Letters* **2009**, *481*, 153-165, 10.1016/j.cplett.2009.09.020.
34. Jinda Lin; Yong-Qing Li; Optical trapping and rotation of airborne absorbing particles with a single focused laser beam. *Applied Physics Letters* **2014**, *104*, 101909, 10.1063/1.4868542.
35. Zhiyong Gong; Yong-Le Pan; Chuji Wang; Optical configurations for photophoretic trap of single particles in air. *Review of Scientific Instruments* **2016**, *87*, 103104, 10.1063/1.4963842.
36. Anton S. Desyatnikov; Vladlen G. Shvedov; Andrei V. Rode; Wieslaw Krolikowski; Yuri S. Kivshar; Photophoretic manipulation of absorbing aerosol particles with vortex beams: theory versus experiment. *Optics Express* **2009**, *17*, 8201-8211, 10.1364/oe.17.008201.
37. J. C. Tung; Y. Y. Ma; Katsuhiko Miamoto; Yi-Fan Chen; Takashige Omatsu; Bottle beam generation from a frequency-doubled Nd:YVO4 laser. *Scientific Reports* **2018**, *8*, 16576, 10.1038/s41598-018-34783-z.
38. John Paul Spence; G Subramanian; P Musumeci; Hollow cone illumination for fast TEM, and outrunning damage with electrons. *Journal of Physics B: Atomic, Molecular and Optical Physics* **2015**, *48*, 214003, 10.1088/0953-4075/48/21/214003.
39. Fengrui Liu; Zhigang Zhang; Yufeng Wei; Qingchuan Zhang; Teng Cheng; Xiaoping Wu; Photophoretic trapping of multiple particles in tapered-ring optical field.. *Optics Express* **2014**, *22*, 23716-23723, 10.1364/oe.22.023716.
40. Pawel Karpinski; Steven Jones; Daniel Andrén; Mikael Käll; Counter-Propagating Optical Trapping of Resonant Nanoparticles Using a Uniaxial Crystal. *Laser & Photonics Reviews* **2018**, *12*, 1800139, 10.1002/lpor.201800139.
41. Ashkin, A.; Optical trapping and manipulation of meutral particles using lasers. *Proc. Natl. Acad. Sci. USA* **1997**, *94*, 4853–4860, .
42. Brandon Redding; Steven C. Hill; Dimitri Alexson; Chuji Wang; Yong-Le Pan; Photophoretic trapping of airborne particles using ultraviolet illumination. *Optics Express* **2015**, *23*, 3630, 10.1364/oe.23.003630.
43. Brandon Redding; Yong-Le Pan; Optical trap for both transparent and absorbing particles in air using a single shaped laser beam. *Optics Letters* **2015**, *40*, 2798-2801, 10.1364/ol.40.002798.
44. Dear, R.; Burnham, D.; Summers, M.; McGloin, D.; Ritchie, G.; Single aerosol trapping with an annular beam improved particle localization. *Phys. Chem. Chem. Phys.* **2012**, *14*, 15826–15831, .
45. G. Roosen; C. Imbert; Optical levitation by means of two horizontal laser beams: A theoretical and experimental study. *Physics Letters A* **1976**, *59*, 6-8, 10.1016/0375-9601(76)90333-9.
46. M E Lewittes; S J Arnold; George Oster; Radiometric levitation of micron sized spheres. *Applied Physics Letters* **1982**, *40*, 455-457, 10.1063/1.93146.
47. Courvoisier, F.; Zhang, J.; Bhuyan, M.K.; Jacquot, M.; Dudley, J.M. Applications of femtosecond Bessel beams to laser ablation. Appl. Phys. A 2013, 112, 29–34.
48. Duocastella, M.; Arnold, C.B. Bessel and annular beams for material processing. Laser Photonics Rev. 2012, 5, 607–621.
49. Stoian, R.; Bhuyan, M.K.; Zhang, G.; Cheng, G.; Meyer, R.; Courvoisier, F. Ultrafast Bessel beams: Advanced tools for laser materials processing. Adv. Opt. Technol. 2018, 7, 165–174.
50. Merano, M.; Boyer, G.; Trisorio, A.; Cheriaux, G.; Mourou, G. Superresolved femtosecond laser ablation. Opt. Lett. 2007, 32, 2239–2241.
51. Butt, M.A.; Nguyen, H.-D.; Rodenas, A.; Romero, C.; Moreno, P.; De Aldana, J.; Aguilo, M.; Sole, R.; Pujol, M.; Diaz, F. Low-repitition rate femtosecond laser writing of optical waveguides in KTP crystals: Analysis of anisotropic refractive index changes. Opt. Express 2015, 23, 15343–15355.
52. Sugioka, K.; Cheng, Y. Ultrafast lasers-reliable tools for advanced materials processing. Light Sci. Appl. 2014, 3, e149.

53. Liu, P.; Jiang, L.; Hu, J.; Yan, X.; Xia, B.; Lu, Y. Etching rate enhancement by shaped femtosecond pulse train electron dynamics control for microchannels fabrication in fused silica glass. Opt. Lett. 2013, 38, 4613–4616.

54. Vishnubhatla, K.; Bellini, N.; Ramponi, R.; Cerullo, G.; Osellame, R. Shape control of microchannels fabricated in fused silica by femtosecond laser irradiated and chemical etching. Opt. Express 2009, 17, 8685–8695.

55. Wang, Z.; Jiang, L.; Li, X.; Wang, A.; Yao, Z.; Zhang, K.; Lu, Y. High-throughput microchannel fabrication in fused silica by temporally shaped femtosecond laser Bessel-beam-assisted chemical etching. Opt. Lett. 2018, 43, 98–101.

56. Xiuxiang Chu; Quan Sun; Jing Wang; Pin Lü; Wenke Xie; Xiaojun Xu; Generating a Bessel-Gaussian beam for the application in optical engineering. *Scientific Reports* **2015**, *5*, 18665, 10.1038/srep18665.

57. Mindaugas Mikutis; Tadas Kudrius; Gintas Šlekys; Domas Paipulas; Saulius Juodkazis; High 90% efficiency Bragg gratings formed in fused silica by femtosecond Gauss-Bessel laser beams. *Optical Materials Express* **2013**, *3*, 1862-1871, 10.1364/ome.3.001862.

58. M. K. Bhuyan; François Courvoisier; P.-A. Lacourt; M. Jacquot; L. Furfaro; M. J. Withford; J. M. Dudley; High aspect ratio taper-free microchannel fabrication using femtosecond Bessel beams. *Optics Express* **2010**, *18*, 566-574, 10.1364/oe.18.000566.

59. Liang Yang; Ayman El-Tamer; Ulf Hinze; Jiawen Li; Yanlei Hu; Wenhao Huang; Jiaru Chu; Boris N. Chichkov; Two-photon polymerization of cylinder microstructures by femtosecond Bessel beams. *Applied Physics Letters* **2014**, *105*, 041110, 10.1063/1.4891841.

60. Slevas, P.; Orlov, S.; Nacius, E.; Ulcinas, O.; Gotovski, P.; Baltrukonis, J.; Jukna, V. Laser induced modifications in transparent materials using azimuthally modulated axicon beams. In Proceedings of the SPIE 11267, Laser Applications in Microelectronic and Optoelectronic Manufacturing (LAMOM) XXV, 112670B, San Francisco, CA, USA, 2 March 2020.

61. Baltrukonis, J.; Ulcinas, O.; Gotovski, P.; Orlov, S.; Jukna, V. Realization of higher order vector Bessel beams for transparent material processing applications. In Proceedings of the SPIE 11268, Laser-based Micro- and Nanoprocessing XIV, 112681D, San Francisco, CA, USA, 2 March 2020.

62. Chongshen Song; Zheyao Wang; Qianwen Chen; Jian Cai; Litian Liu; High aspect ratio copper through-silicon-vias for 3D integration. *Microelectronic Engineering* **2008**, *85*, 1952-1956, 10.1016/j.mee.2008.05.017.

63. B Tan; Deep micro hole drilling in a silicon substrate using multi-bursts of nanosecond UV laser pulses. *Journal of Micromechanics and Microengineering* **2005**, *16*, 109-112, 10.1088/0960-1317/16/1/015.

64. Fei He; Han Xu; Y. Cheng; Jielei Ni; Hui Xiong; Zhizhan Xu; Koji Sugioka; Katsumi Midorikawa; Fabrication of microfluidic channels with a circular cross section using spatiotemporally focused femtosecond laser pulses. *Optics Letters* **2010**, *35*, 1106-1108, 10.1364/ol.35.001106.

65. N. Bärsch; K. Körber; A. Ostendorf; K.H. Tönshoff; Ablation and cutting of planar silicon devices using femtosecond laser pulses. *Applied Physics A* **2003**, *77*, 237-242, 10.1007/s00339-003-2118-4.

66. He, F.; Yu, J.; Chu, W.; Wang, Z.; Tan, Y.; Cheng, Y.; Sugioka, K. Tailored femtosecond Bessel beams for high-throughput, taper-free through-Silicon vias (TSVs) fabrication. In Proceedings of the SPIE 9735, 973506–1, San Francisco, CA, USA, 14 March 2016.

67. Fei He; Junjie Yu; Yuanxin Tan; Wei Chu; Changhe Zhou; Ya Cheng; Koji Sugioka; Tailoring femtosecond 1.5-μm Bessel beams for manufacturing high-aspect-ratio through-silicon vias. *Scientific Reports* **2017**, *7*, 40785, 10.1038/srep40785.

68. Shuhui Li; Jian Wang; Adaptive free-space optical communications through turbulence using self-healing Bessel beams. *Scientific Reports* **2017**, *7*, 43233, 10.1038/srep43233.

69. Zdenÿek Bouchal; Nondiffracting Optical Beams: Physical Properties, Experiments, and Applications. *Czechoslovak Journal of Physics* **2003**, *53*, 537-578, 10.1023/a:1024802801048.

70. Wiersma, N. Photorefractive Self-Focusing of Airy Beams: Nonlinear Interactions and All-Optical Waveguiding. Ph.D. Thesis, Universite de Lorraine, Nancy, France, 2016.

71. Christian Vetter; Ralf Steinkopf; Klaus Bergner; Marco Ornigotti; Stefan Nolte; Herbert Gross; Alexander Szameit; Realization of Free-Space Long-Distance Self-Healing Bessel Beams. *Laser & Photonics Reviews* **2019**, *13*, 1900103, 10.1002/lpor.201900103.

72. Kaushal, H.; Kaddoum, G. Underwater optical wireless communication. IEEE Access 2016, 4, 1518–1547.

73. Saeed, N.; Celik, A.; Al-Naffouri, T.Y.; Alouini, M.-S. Underwater optical wireless communications, networking, and localization: A survey. Ad Hoc Netw. 2019, 94, 101935.

74. Spagnolo, G.S.; Cozzella, L.; Leccese, F. Underwater optical wireless communications: Overview. Sensors 2020, 20, 2261.

75. Jia Xu; Daomu Zhao; Propagation of a stochastic electromagnetic vortex beam in the oceanic turbulence. *Optics & Laser Technology* **2014**, *57*, 189-193, 10.1016/j.optlastec.2013.10.019.

76. Yongping Huang; Zhang Bin; Zenghui Gao; Guangpu Zhao; Zhichun Duan; Evolution behavior of Gaussian Schell-model vortex beams propagating through oceanic turbulence. *Optics Express* **2014**, *22*, 17723-17734, 10.1364/oe.22.017723.

77. Xiang, Y.; Zheng, R.; Yue, P.; Ding, W.; Shen, C. Propagation properties of OAM modes carried by partially coherent LG beams in turbulent ocean based on an oceanic power-law spectrum. Opt. Commun. 2019, 443, 238–244.

78. Cheng, M.; Guo, L.; Li, J.; Huang, Q.; Cheng, Q.; Zhang, D. Propagation of an optical vortex carried by a partially coherent Laguerre-Gaussian beam in turbulent ocean. Appl. Opt. 2016, 55, 4642–4648.

79. Mingjian Cheng; Lixin Guo; Jiangting Li; Yixin Zhang; Channel Capacity of the OAM-Based Free-Space Optical Communication Links With Bessel–Gauss Beams in Turbulent Ocean. *IEEE Photonics Journal* **2016**, *8*, 1-11, 10.1109/jphot.2016.2518865.

80. Jun Ou; Yuesong Jiang; Jiahua Zhang; Hua Tang; Yuntao He; Shuaihui Wang; Jilan Liao; Spreading of spiral spectrum of Bessel–Gaussian beam in non-Kolmogorov turbulence. *Optics Communications* **2014**, *318*, 95-99, 10.1016/j.optcom.2013.12.069.

81. Shengmei Zhao; Wenhao Zhang; Le Wang; Wei Li; Longyan Gong; Weiwen Cheng; Hanwu Chen; Jozef Gruska; Propagation and self-healing properties of Bessel-Gaussian beam carrying orbital angular momentum in an underwater environment. *Scientific Reports* **2019**, *9*, 1-8, 10.1038/s41598-018-38409-2.

82. Willner, A.; Zhao, Z.; Ren, Y.; Li, L.; Xie, G.; Song, H.; Liu, C.; Zhang, R.; Bao, C.; Pang, K. Underwater optical communications using orbital angular momentum-based spatial division multiplexing. Opt. Commun. 2018, 408, 21–25.

83. Fu, S.; Gao, C. Influence of atmospheric turbulence effetcs on the orbital angular momentum spectra of vortex beams. Photonics Res. 2016, 4, B1.

84. Kaicheng Zhu; Guoquan Zhou; Xuguang Li; Xiaojuan Zheng; Huiqin Tang; Propagation of Bessel-Gaussian beams with optical vortices in turbulent atmosphere. *Optics Express* **2008**, *16*, 21315-21320, 10.1364/oe.16.021315.

85. Jing Du; Jian Wang; High-dimensional structured light coding/decoding for free-space optical communications free of obstructions. *Optics Letters* **2015**, *40*, 4827-4830, 10.1364/ol.40.004827.

86. James G. Fujimoto; Costas Pitris; Stephen A. Boppart; Mark E. Brezinski; Optical Coherence Tomography: An Emerging Technology for Biomedical Imaging and Optical Biopsy. *Neoplasia* **2000**, *2*, 9-25, 10.1038/sj.neo.7900071.

87. Tuqiang Xie; Shuguang Guo; Zhongping Chen; David Mukai; Matthew Brenner; GRIN lens rod based probe for endoscopic spectral domain optical coherence tomography with fast dynamic focus tracking. *Optics Express* **2006**, *14*, 3238-3246, 10.1364/oe.14.003238.

88. S. Murali; K. S. Lee; J. P. Rolland; Invariant resolution dynamic focus OCM based on liquid crystal lens.. *Optics Express* **2007**, *15*, 15854-15862, 10.1364/oe.15.015854.

89. Tetsu Asami; Hiroko Terasaki; Yasuki Ito; Tadasu Sugita; Hiroki Kaneko; Junpei Nishiyama; Hajime Namiki; Masahiko Kobayashi; Norihiko Nishizawa; Development of a Fiber-Optic Optical Coherence Tomography Probe for Intraocular Use. *Investigative Opthalmology & Visual Science* **2016**, *57*, OCT568-OCT574, 10.1167/iovs.15-18853.

90. John H. McLeod; The Axicon: A New Type of Optical Element. *Journal of the Optical Society of America* **1954**, *44*, 592-592, 10.1364/josa.44.000592.

91. Lorenser, D.; Singe, C.; Curatolo, A.; Sampson, D. Energy-efficient low-Fresnel-number Bessel beams and their application in optical coherence tomography. Opt. Lett. 2014, 39, 548–551.

92. Yi, L.; Sun, L.; Ding, W. Multifocal spectral-domain optical coherence tomography based on Bessel beam for extended imaging depth. J. Biomed. Opt. 2017, 22, 106016.

93. Biwei Yin; Chulho Hyun; Joseph A. Gardecki; Guillermo J. Tearney; Extended depth of focus for coherence-based cellular imaging. *Optica* **2017**, *4*, 959-965, 10.1364/optica.4.000959.

94. Zhihua Ding; Hongwu Ren; Yonghua Zhao; J. Stuart Nelson; Zhongping Chen; High-resolution optical coherence tomography over a large depth range with an axicon lens. *Optics Letters* **2002**, *27*, 243-245, 10.1364/ol.27.000243.

95. R. A. Leitgeb; M Villiger; A H Bachmann; L Steinmann; T Lasser; Extended focus depth for Fourier domain optical coherence microscopy.. *Optics Letters* **2006**, *31*, 2450–2452, .

96. Kye-Sung Lee; Jannick P. Rolland; Bessel beam spectral-domain high-resolution optical coherence tomography with micro-optic axicon providing extended focusing range. *Optics Letters* **2008**, *33*, 1696-1698, 10.1364/ol.33.001696.

97. Arlt, J.; Dholakia, K. Generation of high-order Bessel beams by use of an axicon. Opt. Commun. 2000, 177, 297–301.
98. McGloin, D.; Dholakia, K. Bessel beams: Diffraction in a new light. Contemp. Phys. 2005, 46, 15–28.
99. K. M. Tan; M Mazilu; T. H. Chow; W M Lee; K Taguichi; B K Ng; W. Sibbett; C S Herrington; C. T. A. Brown; Kishan Dholakia; et al. In-fiber common-path optical coherence tomography using a conical-tip fiber.. *Optics Express* **2009**, *17*, 2375–2384, .
100. Schwarz, S.; Roth, G.-L.; Rung, S.; Esen, C.; Hellmann, R. Fabrication and evaluation of negative axicons for ultrashort pulsed laser applications. Opt. Express 2020, 28, 26207–26217.
101. Ruan, H.; Wang, L.; Wu, S.; Liu, L.; Zhou, B. Free space vortex light by diffraction of a Bessel Beam from Optical Fiber. IEEE Photonics J. 2017, 9, 1–10.
102. Kaushal Vairagi; Rashmi A. Minz; Sarabjeet Kaur; Dharmadas Kumbhakar; Sambhav Paul; Umesh K. Tiwari; Ravindra Kumar Sinha; Jochen Fick; Samir K. Mondal; Deep Seated Negative Axicon in Selective Optical Fibre Tip and Collimated Bessel Beam. *IEEE Photonics Technology Letters* **2017**, *29*, 786–789, 10.1109/LPT.2017.2684224.
103. Florian Stuker; Jorge Ripoll; Markus Rudin; Fluorescence Molecular Tomography: Principles and Potential for Pharmaceutical Research. *Pharmaceutics* **2011**, *3*, 229-274, 10.3390/pharmaceutics3020229.
